15 May 2023

A Prediction of Young's Modulus for Tin Containing Phosphate Glasses using Quantitative Structural Information

Tatsuki Shimizu

Akira Saitoh

Uwe Hoppe

Grégory Tricot

et. al. For a complete list of authors, see https://scholarsmine.mst.edu/matsci_eng_facwork/2922

Recommended Citation

T. Shimizu et al., "A Prediction of Young's Modulus for Tin Containing Phosphate Glasses using Quantitative Structural Information," *Journal of Non-Crystalline Solids*, vol. 608, article no. 122262, Elsevier, May 2023.
The definitive version is available at https://doi.org/10.1016/j.jnoncrysol.2023.122262

Journal of Non-Crystalline Solids 608 (2023) 122262

Contents lists available at ScienceDirect

Journal of Non-Crystalline Solids

journal homepage: www.elsevier.com/locate/jnoncrysol

A prediction of Young's modulus for tin containing phosphate glasses using quantitative structural information

Tatsuki Shimizu [a], Akira Saitoh [a,*], Uwe Hoppe [b], Grégory Tricot [c], Richard K. Brow [d]

[a] Graduate School of Science and Engineering, Ehime University, Matsuyama, Ehime 790-8577, Japan
[b] Institut für Physik, Universität Rostock, Rostock 18051, Germany
[c] Université de Lille, CNRS, UMR 8516, LASIR-Laboratoire de Spectrochimie Infrarouge et Raman, Lille F-59000, France
[d] Department of Materials Science and Engineering, Missouri University of Science and Technology, Rolla, MO 65409, United States

ARTICLE INFO

Keywords:
Tin phosphate glass
Young's modulus
X-ray/neutron diffraction
31P MAS-NMR
Short-range structure

ABSTRACT

A rigid unit packing fraction (RUPF) model was used to better understand the influence of local structural units on the Young's elastic modulus (E) of binary and ternary tin phosphate glasses. Quantitative analyses of the units that constitute the glass structure, obtained from X-ray/neutron diffraction and ^{31}P MAS-NMR spectroscopy, were used to calculate polyhedral packing fractions that, with tabulated bond dissociation energies, were used to predict E based on a modification of the Makashima-Mackenzie relationship, which uses ion sizes to calculate packing fractions. Predictions based on the RUPF model are better than those based on ion sizes, and extending the RUPF model to all cation-polyhedra accounts for the compositional dependence of the Sn-coordination number.

1. Introduction

The elastic modulus of an oxide glass depends on the nature of the bonds that constitute the glass structure and the ability to predict elastic modulus aids in the design of glass compositions with specific properties [1]. Makishima and Mackenzie (MM) [2] developed a model to predict Young's modulus, E, by considering the electrostatic attraction between oxide ions and metal cations and the atomic packing fraction of those ions, V_p, according to

$$E = 2V_p\sum_i G_i X_i \quad (1)$$

where G_i is the dissociation energy per unit volume of the oxide component "i" and X_i is the oxide molar fraction, calculated from tabulated ion sizes. Inaba et al. [3] noted that the use of oxide dissociation energies did not properly account for the different types of bonds associated with glass-forming oxides like B_2O_3, P_2O_5 and SiO_2. They modified the MM model using dissociation energies that were calculated from the number of oxygen bonds that link a metal cation to a neighboring cation. For example, the $P=O$ double-bond in the tetrahedra that constitute the structure of P_2O_5 was not considered a coordinating bond and so was not considered when calculating the dissociation energy per bond contributed by the phosphate component of a glass. As a result, the predictions of the Young's modulus by Inaba et al. [3] were much closer to the measured values, particularly for phosphate glasses, than those that relied on the oxide dissociation energies used in the MM model.

In a recent study of the mechanical properties of Zn-Sn-phosphate glasses by Okamoto et al. [4], the Inaba model was modified by using metal-oxygen bond distances and metal-ion coordination numbers, determined from X-ray and neutron diffraction studies [5–7], to calculate ionic packing fractions (V_p). In addition, Okamoto et al. modified the dissociation energies used by Inaba et al. to account for different coordination environments, particularly for the Sn^{2+}-polyhedra, and to account for the greater rigidity of isolated PO_4^{3-} (Q^0) tetrahedra, compared to tetrahedra that link to neighboring P-tetrahedra through one (Q^1) or two (Q^2) bridging oxygen bonds. Okamoto's new values for individual oxide dissociation energy and volume yielded improved predictions of the elastic moduli and Vickers hardness of several series of xZnO−(67−x)SnO−33P_2O_5 glasses, compositions with useful photoelastic properties [4].

More recently, Shi et al. [8] have revisited the MM-model by noting that the effective volumes of the metal-polyhedra that constitute the structures of oxide glasses are not the summation of the ionic radii that constitute a polyhedron but must also include the unoccupied space within that polyhedron. By replacing the atomic packing fraction in the

* Corresponding author.
E-mail address: asaito@ehime-u.ac.jp (A. Saitoh).

https://doi.org/10.1016/j.jnoncrysol.2023.122262
Received 4 January 2023; Received in revised form 10 February 2023; Accepted 27 February 2023
Available online 4 March 2023

Table 1
Methods used to calculate Young's modulus from parameters related to individual bond strengths and ion packing.

	Makishima-Mackenzie [2]	Inaba [3]	Okamoto [4]	Shi [8]	Current Study (Shimizu)
Bond Strength Parameter	Oxide dissociation energy	Diss. energy normalized to CN	Diss. energy with Q^0-adjustment	Best-fit dissociation energies	Okamoto dissociation energies
Ion Packing Parameter	Individual ion size	Individual ion size	Bond lengths, CN, diffraction	RUPF for glass-forming polyhedra	RUPF for all polyhedra

MM-model with the Rigid Unit Packing Fraction (RUPF) of the network polyhedra, Shi et al. were able to significantly improve their predictions of the elastic moduli of many different series of oxide glasses.

Shi et al. used the isolated volumes of modifying cations in their calculations of ionic packing fractions and did not consider the unoccupied space associated with modifier polyhedra. In the present study, RUPF calculations for glass-forming and modifying polyhedra have been made using with metal-oxygen bond distances and coordination numbers determined from earlier diffraction studies, along with the dissociation energies calculated by Okamoto et al. using P-tetrahedral Q-distributions from ^{31}P NMR studies, to predict the elastic moduli of ternary Zn-Sn-phosphate and Ba-Sn-phosphate glasses of interest for photoelastic applications. Applying the RUPF calculations to every polyhedron that constitutes a glass structure provides a better prediction of elastic modulus than previous approaches.

2. Experimental procedures

The preparation conditions, compositions, and elastic moduli of the $SnO-P_2O_5$, $ZnO-SnO-P_2O_5$, and $BaO-SnO-P_2O_5$ glasses are reported elsewhere [6,9–11] and are summarized in Table A1. In general, glasses were prepared from the appropriate mixtures of reagent grade raw materials melted in carbon crucible in a reducing environment to prevent the oxidation of Sn^{2+} to Sn^{4+} [12]. This oxidation is unwanted because it will create additional non-bridging oxygens and will significantly shorten the phosphate chains. The glasses are X-ray amorphous and their compositions were determined using energy dispersive SEM-EDS with an uncertainty of 0.1–2 mol%, depending on the sample. Densities were determined using the Archimedes method with kerosene as the buoyancy fluid. Three bubble-free samples of each composition were analyzed, and the average values are reported. Young's modulus measurements were made using an ultrasonic system equipped with a 10 MHz transducer, unless noted otherwise; these values were reproducible to ± 2 GPa.

Quantitative structural information was obtained from diffraction studies [5–7] and the ^{31}P magic angle spinning nuclear magnetic resonance experiments [5,7,13] described elsewhere. That information is summarized in Table A2. The conversion of this structural information into parameters used to predict the compositional dependence of Young's modulus is described below.

3. Results and discussion

Table 1 summarizes different calculations for the compositional dependences of the Young's modulus of oxide glasses. Each of these calculations are based on variations of Eq. (1), from Makishima-Mackenzie [2], which assumes that the Young's modulus of a glass can be calculated from the individual bond strengths of oxides that constitute the composition of a glass and from the packing efficiency of the ions contributed by those oxides. Makishima and Mackenzie calculated the individual bond strengths from the respective oxide dissociation energies and used tabulated ion sizes to calculate packing efficiencies. Inaba et al. [3] modified the calculation of dissociation energy per bond by considering the number of bridging oxygens per metal instead of its coordination number. Hoppe et al. [6] modified the Inaba approach by using ion sizes calculated from bond distances and metal-oxygen coordination numbers directly obtained from diffraction analyses to calculate the ion packing ratio and the dissociation energy per bond. Okamoto also modified the average dissociation energy calculation for P_2O_5 by assuming that bridging oxygens between two P-tetrahedra created some structural flexibility that does not exist for anionic orthophosphate (Q^0) units. Sun and Huggins took a similar approach when calculated the molar dissociation energy for silica, using a greater dissociation energy for silica in Ca_2SiO_4 than in SiO_2 [14]. Okamoto et al. then used quantitative ^{31}P NMR to calculate the relative concentrations of different phosphate sites to calculate elastic modulus [4].

Shi et al. [8] realized that packing fractions based on ion sizes underestimated the effect of ion packing on the elastic modulus because those calculations did not account for the unoccupied interstitial space between the ions in a polyhedron. If that volume is included, then the effective packing volume of a polyhedron is greater than that of the sum of the volumes of the individual ions in that polyhedron, and so, through Eq. (1), these rigid units would contribute more to the calculated elastic modulus. Fig. 1 shows the schematic representation of the interstitial volume in an isolated polyhedron and one that links to form a larger anion.

Shi et al. also calculated the molar dissociation energies for typical constituents of oxide glasses, using a statistical best-fit approach for the

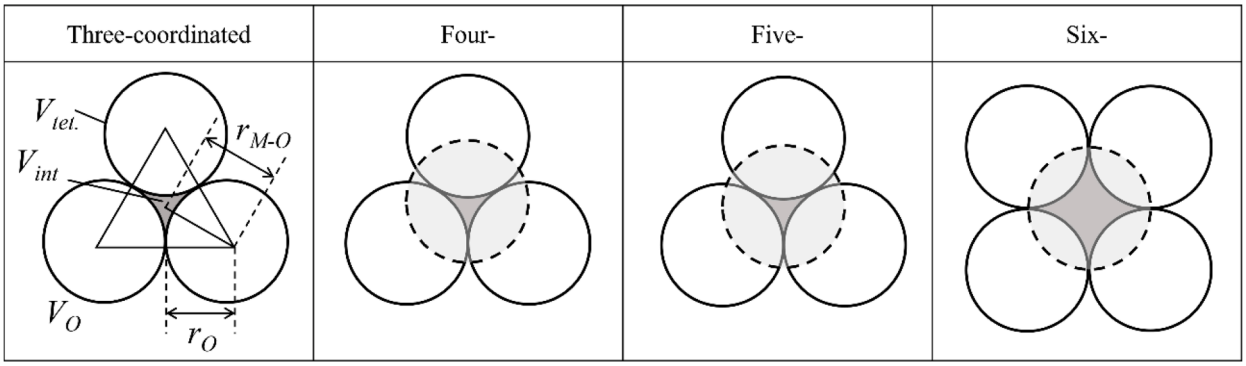

Fig. 1. Schematic illustration of three-, four-, five- and six-coordinated units for the RUPF model. The spheres are cross-sectional representations of the electron clouds of bridging and non-bridging oxygens. gray area denotes an interstitial space.

Table 2
Parameters for the bond length (r) and the molar dissociation energy (G_i) [15] for each oxide used in the calculations of Young's modulus.

Oxide	C. N.	$r_{M\text{-}O}$ (Å)	r_O (Å)	r_M (Å)	$V_{int.}$	V_O (Å^3)	$V_{M,i}$ (Å^3)	G_i (kJ/mol)
BaO	8	2.82	1.27	1.55	—	8.49	10.17	39.5
SnO	3	2.16		0.89			5.28	39.9
	4	2.23		0.96			3.23	39.9
ZnO	4	1.95		0.68			2.98	49.9
	5	2.00		0.73			4.36	49.9
P_2O_5	4	1.55		0.28	0.260		2.98	28.2 (Q^1, Q^2) 56.4 (Q^0)

calculations of elastic moduli for 155 glasses using the modified MM relationship,

$$E = 2 \cdot V_{p,\ RUPF} \cdot \sum_i G_i^{RUPF} X_i \tag{2}$$

Following Shi et al., $V_{p,RUPF}$ was calculated in the present study from the PO_4 tetrahedral volume $V_{tet.}$, the modifier ion volume $V_{mod.}$ and the molar volume of the glass, V_{mol},

$$V_{p,RUPF} = N_A \cdot \frac{V_{tet.} + V_{mod.}}{V_{mol}} \tag{3}$$

Here, N_A is Avogadro's number, and V_{mol} is calculated from the molar weight (MW) of the glass and its density (r),

$$V_{mol} = \frac{MW}{\rho} \tag{4}$$

$V_{tet.}$ was calculated according to:

$$V_{tet.} = 4 \cdot V_O + V_{int.} \tag{5}$$

where V_O is the molecular volume of oxygen ions in a tetrahedron and $V_{int.}$ is the interstitial unoccupied space within a tetrahedron, as calculated from

$$V_{int.} = 0.351 \cdot V_O \tag{6}$$

and

$$V_O = \frac{4}{3} \cdot \pi \cdot r_O^3 \tag{7}$$

Oxygen ion sizes were calculated from the average P–O bond lengths ($r_{p\text{-}o}$) obtained from the diffraction data on the glasses in the present study (Table 2) and by using the "touching" oxygen calculations from the RUPF model:

$$r_o = r_{P-O} \cdot \sqrt{\frac{2}{3}} \tag{8}$$

Those oxygen radii were then used with the metal-oxygen bond distances from the diffraction studies (Table 2) to calculate the metal ion radii (r_M) were then used to calculate the volume of a metal ion ($V_{M,i}$) using

$$V_{M,\ i} = \frac{4}{3} \cdot \pi \cdot r_M^3 \tag{9}$$

The total volume of the metal ions is then calculated from

$$V_{mod.} = N_A \cdot \sum V_{M,i} \cdot X_i \tag{10}$$

It is worth noting here that the RUPF model has been used for both the glass forming oxides (P_2O_5 in the current study) as well as what may be classified as glass-modifying oxides (SnO, ZnO, and BaO). That is, the unoccupied volume associated within every polyhedron that constitutes the glass structure has been included in the calculation of packing fraction. In their original RUPF paper, Shi, et al. assumed that only the volume of individual, isolated modifying cations contributed to V_{mod}. They did not apply the RUPF analysis to the modifying cations. The dissociation energies of the oxides used in the present study are the same as those described in Okamoto et al. [4] and are based on those reported by Sun [14,15]. Note that we have assumed that the bridging angles (O–P–O) between the Q^2 and Q^1 tetrahedra easily deform under pressure, which results in smaller G_i. On the while, the bond-lengths or bond angles can stiffly respond to pressure when pressure is applied to a Q^0 site [4]. Those energies are shown in Table 2.

Fig. 2(a) and (b) compare the differences between the measured and predicted Young's moduli using the Okamoto et al. [4], Inaba et al. [3], and the current (Shimizu) models, for series of xBaO–(67–x)SnO–33P_2O_5 and xBaO–(60–x)SnO–40P_2O_5 glasses, respectively. Note that the Shi model [2] underpredicts E. One reason for the underprediction of the measured Young's modulus (E) by the Shi model may be related to their estimation of r_o using Eq. (8) might be underestimated, which influences the small V_p. The r_o by the present model was taken by observed diffraction data. The predictions of the MM-Inaba, Okamoto, and current models are similar, although the current model does a better job of predicting the Young's modulus of glasses with greater BaO-contents.

Fig. 3(a) and (b) show results of the measured and calculated Young's (E) modulus reported for ternary barium-tin phosphate glasses, using the predictions from the Shimizu, Okamoto, and MM-Inaba models. It might be good choice to predict Young's modulus of phosphate glasses that the RUPF approach combines to the short-range structure information by X-ray/neutron diffraction and ^{31}P MAS-NMR.

Fig. 4(a) and (b) compare the differences between the measured and predicted Young's moduli using the Okamoto et al. [4], Inaba et al. [3],

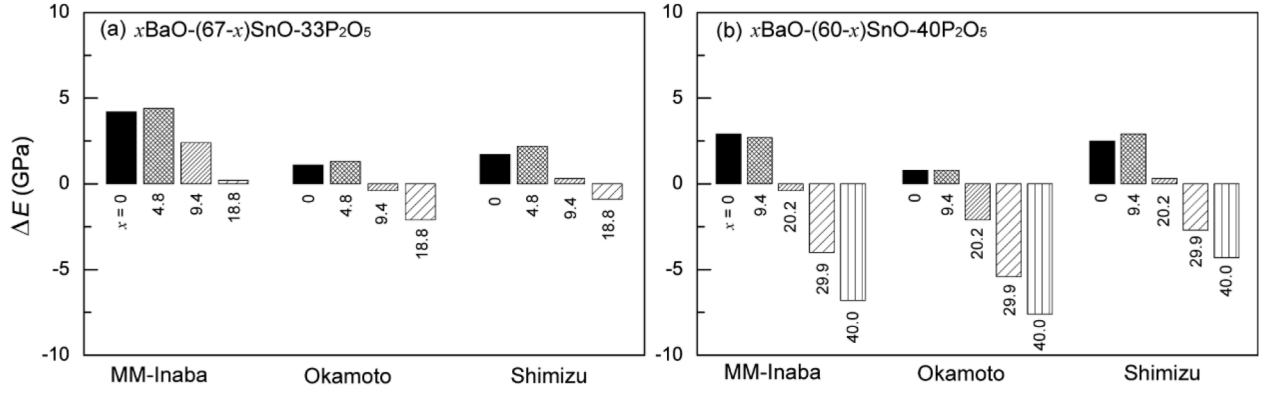

Fig. 2. The difference between the measured Young's modulus and those predicted by the models indicated for series of (a) xBaO–(67–x)SnO–33P_2O_5 and (b) xBaO–(60–x)SnO–40P_2O_5 glasses.

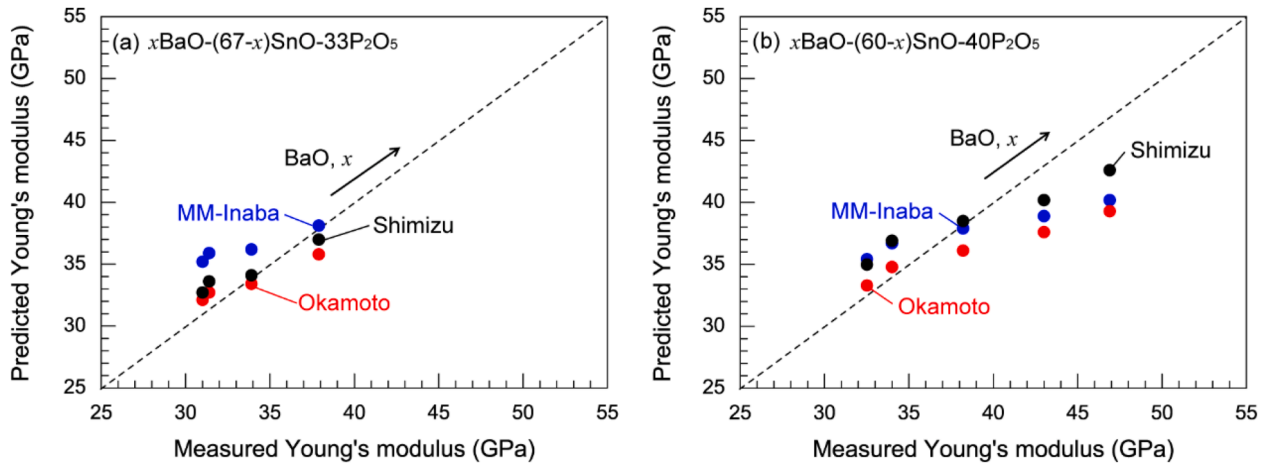

Fig. 3. Young's modulus for measured versus calculated values for the ternary xBaO–(67–x)SnO–33P_2O_5 and xBaO–(60–x)SnO–40P_2O_5 glasses. The structures of these glasses were fully analyzed by X-ray/neutron diffraction [7] and ^{31}P MAS-NMR spectroscopies (Table A1). The black circles are from the current (Shimizu) model, and the red and blue circles are from Okamoto [4] and MM-Inaba [3].

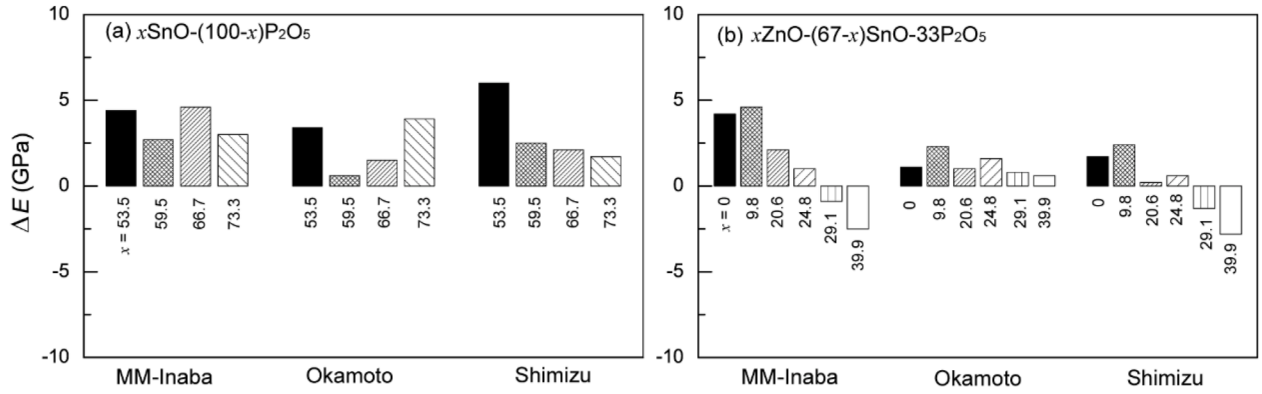

Fig. 4. The difference between the measured Young's modulus and those predicted by the models indicated for series of (a) xSnO–(100–x)P_2O_5 and (b) xZnO–(67–x)SnO–33P_2O_5 [4] glasses.

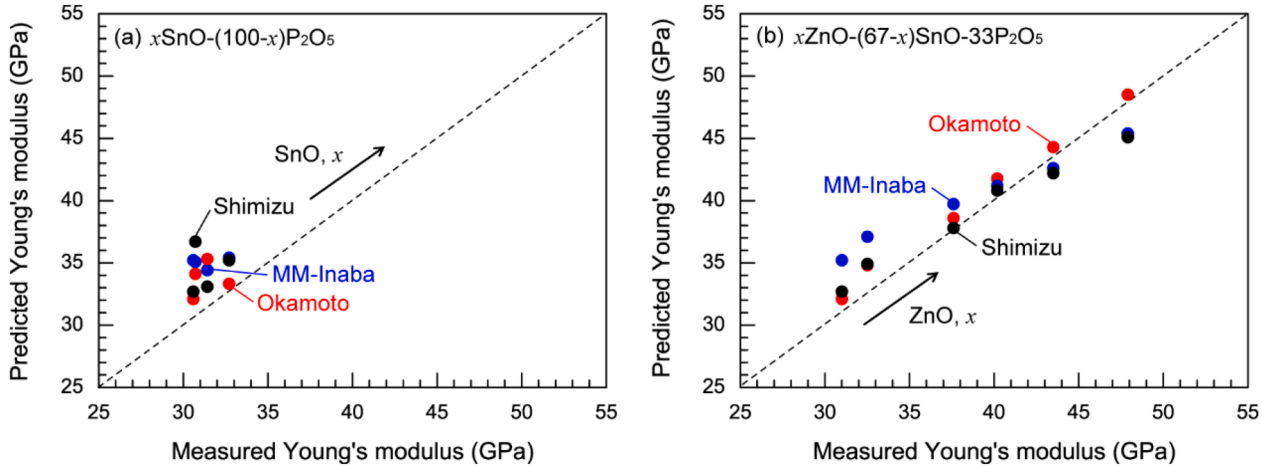

Fig. 5. Young's modulus for measured versus calculated values for the binary (a) xSnO–(100-x)P_2O_5 and the ternary (b) xZnO–(67–x)SnO–33P_2O_5 glasses. The black circles are from the current (Shimizu) model, and the red and blue circles are from MM-Inaba [3] and Okamoto [4].

and the current models, for series of xSnO–(100–x)P_2O_5 and xZnO–(67–x)SnO–33P_2O_5 glasses, respectively. The predictions of the current model for xZnO–(67–x)SnO–33P_2O_5 glasses would be more allowable for the observed Young's modulus of those glasses, although a fluctuation exists in xSnO–(100–x)P_2O_5 glasses.

Fig. 5 shows results of the measured and calculated Young's (E) modulus reported for binary tin and ternary zinc-tin phosphate glasses, using the predictions from the Okamoto et al. [4], Inaba et al. [3], and the current (Shimizu) models. The phosphate glasses are fitted by introducing structural information by X-ray/neutron diffraction [7]. We note that the significant different from the diagonal in the binary SnO–P_2O_5 glasses might be ascribed to observed E, which did not show a compositional evolution.

The prediction of Young's modulus of binary and ternary phosphate glasses by RUPF method reflects short-range structure of intra phosphate tetrahedra, compared to the MM-Inaba-Okamoto methods. Also to be noted is that pyro-phosphate systems tend to fit to the observed Young's modulus. The difference between the two is not a large, that is, to count an interstitial region to estimate V_p among the P-tetrahedral unit in the RUPF. Thereby, the consideration of cationic (bond length and oxygen coordination number) and anionic (manner of phosphate chain) local structure is significant, despite of high-cost experiments being needed.

The RUPF methodology to calculate the modifying polyhedral volumes is limited to be applied, because the oxygen ion sizes were fixed through the touching sphere [8] analysis of the glass-forming polyhedra, so the modifier ion sizes, not polyhedral volumes, have been inevitably used. However, oxygen coordination number is not explicitly used in the RUPF model but the Okamoto model. Furthermore, interstitial volumes caused by pyramidal ($Sn^{2+\,[3]}$) and bi-pyramidal ($Sn^{2+\,[4]}$) [6], distorted octahedral ($Zn^{2+\,[5]}$) [5], and octahedral ($Ba^{2+\,[8]}$) [7] units are indeed included. It might be valuable that tetrahedral ($Zn^{2+\,[4]}$) and octahedral ($Zn^{2+\,[6]}$) [13,16,17] units have been also identified in binary zinc phosphate glasses. Hence, better consideration of the oxygen ion size would produce noticeable prediction, which remains to be explored. And the spatial contribution of the Sn^{2+} lone pair, which might require additional space needs to be considered. Other better approach to calculate E value may come from topological constraint theory [18]. However, that works only with several adjusted parameters for individual oxide glasses.

Finally, observed Young's modulus are discussed based on the elucidated coordination structures. In the Zn-Sn ternary system, Sn^{2+} coordination number increases with increasing ZnO concentration. Furthermore, zinc-ortho phosphate subnetwork spreads when high content ZnO [5]. On the contrary in the Ba-Sn systems, Sn^{2+} coordination number slightly increases with increasing BaO concentration (see Table A2) [7]. BaO is obviously larger V_M than ZnO as shown in Table 2. But not large glass formation region in the Ba-Sn phosphate glasses caused by no sub-network structure leads to suppress the larger Young's modulus. High coordinated Sn^{2+} is an advantage for high elastic phosphate glass as well as high refractivity and small photoelasticity.

4. Conclusions

The present study has deduced a new approach to prediction of Young's modulus in the phosphate glasses by the rigid unit packing fraction method that includes the realistic structural information by X-ray/neutron diffraction and ^{31}P MAS-NMR aiming at calculation of ion packing ratio and dissociation energy. The results of this study are summarized as follows:

(1) The RUPF method might validate binary and ternary tin phosphate glasses and reasonably predict the observed Young's modulus of phosphate glasses.
(2) Consistent Young's moduli are calculated when fully structural information with coordination number of oxygens around cation by X-Ray diffraction and Q^n phosphate speciation by ^{31}P NMR are provided.
(3) The difference of calculated Young's modulus between Makishima-Mackenzie and present RUPF methods is not large, despite of taking bond length, coordination number of oxygen, and O/P ratio into account in phosphate glasses. The developed estimation of O-ion sizes belonging to modifier cations would be necessary.

CRediT authorship contribution statement

Tatsuki Shimizu: Data curation. **Akira Saitoh:** Conceptualization, Methodology, Data curation, Writing – original draft. **Uwe Hoppe:** Methodology, Writing – review & editing. **Grégory Tricot:** Data curation, Writing – review & editing. **Richard K. Brow:** Conceptualization, Methodology, Writing – review & editing.

Declaration of Competing Interest

The authors declare that they have no known competing financial interests or personal relationships that could have appeared to influence the work reported in this paper.

Data availability

No data was used for the research described in the article.

Acknowledgment

AS acknowledges the support of the JSPS KAKENHI Grant Number 17K05041.

Appendix

Table A1
Compositional information obtained by SEM-EDS with uncertainty of ±1 mol% and fractions of Q^n ($n = 0, 1, 2$) (n: the number of bridging oxygens on a P-tetrahedron.) determined by ^{31}P MAS-NMR. The uncertainty of fractions is ±0.2. The density data for xZnO–(67–x)SnO–33P_2O_5 glasses are partially from the ref. [4].

(a) xSnO–(100-x)P_2O_5												
Sample	Batched composition (mol%)				Analyzed composition (mol%) by SEM-EDS				Fraction (%) by ^{31}P NMR			
x	ZnO	BaO	SnO	P_2O_5	ZnO	BaO	SnO	P_2O_5	Q^3	Q^2	Q^1	Q^0
53.5	—	—	50	50	—	—	53.5	46.5	0	77.8	22.2	0
59.5			60	40			59.5	40.5	0	54.9	45.1	0
66.7			66.7	33.3			66.7	33.3	0	0.4	93.8	5.8
73.3			72	28			73.3	26.7	0	0	26.1	73.9
(b) xZnO–(67-x)SnO–33P_2O_5												
0	0	—	67	33	0	—	66.7	33.3	0	0.4	93.8	5.8

(continued on next page)

Table A1 (*continued*)

(a) xSnO–(100-x)P_2O_5												
Sample	Batched composition (mol%)				Analyzed composition (mol%) by SEM-EDS				Fraction (%) by ^{31}P NMR			
x	ZnO	BaO	SnO	P_2O_5	ZnO	BaO	SnO	P_2O_5	Q^3	Q^2	Q^1	Q^0
9.8	10		57	33	9.8		57.4	32.8	0	0.5	89.5	9.9
20.6	20		47	33	20.6		46.9	32.5	0	1.2	83.3	15.5
24.8	25		42	33	24.8		42.4	32.8	0	0.5	72.6	26.8
29.1	30		37	33	29.1		38.8	32.1	0	0.8	65.4	33.7
39.9	40		27	33	39.9		28.5	31.6	0	0.2	59.8	40.0
(c) xBaO–(67-x)SnO–33P_2O_5												
0	—	0	67	33	—	0	66.7	33.3	0	0.4	93.8	5.8
4.8		5	62	33		4.8	61.9	33.3	0	4.0	93.0	3.0
9.4		10	57	33		9.4	57.6	33.0	0	7.0	90.0	3.0
18.8		20	47	33		18.8	47.1	34.1	0	12.0	86.0	2.0
(d) xBaO–(60-x)SnO–40P_2O_5												
0	—	0	60	40	—	0	59.5	40.5	0	54.9	45.1	0.0
9.4		10	50	40		9.4	50.2	40.4	0	58.6	41.4	0.0
20.2		20	40	40		20.2	40.0	39.8	0	62.7	37.3	0.0
29.9		30	30	40		29.9	30.3	39.8	0	64.8	35.2	0.0
40.0		40	20	40		40.0	20.1	39.9	0	63.2	36.8	0.0

Table A2
Relevant coordination number, bond length determined by X-ray/neutron diffraction spectroscopy [5–7].

(a) xSnO–(100-x)P_2O_5								
Sample	Coordination number				Bond length (nm)			
x	ZnO	BaO	SnO	P_2O_5	Zn–O	Ba–O	Sn–O	P–O
53.5	—	—	3.9	4.0		—	0.223	0.155
59.5			3.5	4.0			0.218	0.155
66.7			3.1	4.0			0.216	0.155
73.3			3.3	4.0			0.217	0.155
(b) xZnO–(67-x)SnO–33P_2O_5								
0	0	—	3.1	4.0	0.200	—	0.216	0.155
9.8	4.7		3.2	4.0	0.195		0.217	0.155
20.6	4.4		3.3	4.0	0.198		0.218	0.155
24.8	4.6		3.5	4.0	0.200		0.222	0.155
29.1	4.4		3.7	4.0	0.199		0.222	0.155
39.9	4.4		3.9	4.0	0.200		0.223	0.155
(c) xBaO–(67-x)SnO–33P_2O_5								
0	—	8.0	3.1	4.0	—	0.282	0.215	0.155
4.8		8.0	3.1	4.0		0.282	0.217	0.155
9.4		8.0	3.2	4.0		0.282	0.217	0.155
18.8		8.0	3.2	4.0		0.282	0.218	0.155
(d) xBaO–(60-x)SnO–40P_2O_5								
0	—	8.0	3.5	4.0	—	0.282	0.216	0.155
9.4		8.0	3.4	4.0		0.282	0.217	0.155
20.2		8.0	3.3	4.0		0.282	0.217	0.155
29.9		8.0	3.3	4.0		0.282	0.217	0.155
40.0		8.0	3.4	4.0		0.282	0.216	0.156

References

[1] T. Rouxel, Elastic properties and short-to medium-range order in glasses, J. Amer. Ceram. Soc. 90 (2007) 3019–3039.

[2] A. Makishima, J.D. Mackenzie, Direct calculation of Young's modulus of glass, J. Non Cryst. Solids 12 (1973) 35–45.

[3] S. Inaba, S. Fujino, K. Morinaga, Young's modulus and compositional parameters of oxide glasses, J. Amer. Ceram. Soc. 82 (1999) 3501–3507.

[4] T. Okamoto, A. Saitoh, P. Freudenberger, H. Takebe, R.K. Brow, The structure and properties of xZnO–(67–x)SnO–33P_2O_5 glasses: (IV) mechanical properties, J. Non Cryst. Solids 513 (2019) 44–48.

[5] U. Hoppe, A. Saitoh, G. Tricot, P. Freudenberger, A.C. Hannon, H. Takebe, R. K. Brow, The structure and properties of xZnO–(67-x)SnO–33P_2O_5 glasses: (II) diffraction, NMR, and chromatographic studies J, Non Cryst. Solids 492 (2018) 68–76.

[6] U. Hoppe, R.K. Brow, A.C. Hannon, M.V. Zimmermann, Structure of tin phosphate glasses by neutron and X-ray diffraction, J. Non Cryst. Solids X 2 (2019), 100017.

[7] U. Hoppe, A. Saitoh, T. Shimizu, G. Tricot, A.C. Hannon, Properties and structure of ternary BaO-SnO-P_2O_5 glasses, J. Non Cryst. Solids 597 (2022) 1219091–12190910.

[8] Y. Shi, A. Tandia, B. Deng, S.R. Elliott, M. Bauchy, Revisiting the Makishima–Mackenzie model for predicting the Young's modulus of oxide glasses, Acta Mater. 195 (2020) 252–262.

[9] A.A. Higazy, B. Bridge, A. Hussein, M.A. Ewaida, Elastic constants and structure of the vitreous system ZnO–P_2O_5, J. Acous. Soc. Amer. 86 (1989) 1453–1458.

[10] A. Saitoh, R.K. Brow, U. Hoppe, G. Tricot, S. Anan, H. Takebe, The structure and properties of xZnO–(67-x)SnO–33P_2O_5 glasses: (I) optical and thermal properties, infrared and Raman spectroscopies, J. Non Cryst. Solids 484 (2018) 132–138.

[11] M. Itadani, G. Tricot, B. Doumert, H. Takebe, A. Saitoh, Structure and properties of barium tin boro-phosphate glass systems with very low photoelastic constant, J. Appl. Phys. 122 (8) (2017) 08510201–08510210.

[12] H. Segawa, S. Inoue, K. Nomura, Electronic states of SnO-ZnO–P_2O_5 glasses and photoluminescence properties, J. Non Cryst. Solids 358 (11) (2012) 1333–1338.

[13] R.K. Brow, D.R. Tallant, S.T. Myers, C.C. Phifer, The short-range structure of zinc polyphosphate glass, J. Non Cryst. Solids 191 (1995) 45–55.

[14] K.H. Sun, M.L. Huggins, Energy additivity in oxygen-containing crystals and glasses, J. Phys. Colloid Chem. 51 (2) (1947) 438–443.

[15] I.I.K.-H. Sun, M.L. Huggins, Energy additivity in oxygen-containing crystals and glasses II, J. Phys. Colloid Chem. 51 (2) (1947) 438–443.

[16] U. Hoppe, A structural model for phosphate glasses, J. Non Cryst. Solids 195 (1996) 138–147.

[17] U. Hoppe, G. Walter, R. Kranold, D. Stachel, Structural specifics of phosphate glasses probed by diffraction methods: a review, J. Non Cryst. Solids 263 (2000) 29–47. -264.

[18] C.J. Wilkinson, Q. Zheng, L. Huang, J.C. Mauro, Topological constraint model for the elasticity of glass-forming systems, J. Non Cryst. Solids X 2 (2019), 100019.